

C.P. No. 260

(17,784)

A.R.C. Technical Report

C.P. No. 260

(17,784)

A.R.C. Technical Report



MINISTRY OF SUPPLY

AERONAUTICAL RESEARCH COUNCIL

CURRENT PAPERS

Flutter Calculations on a Resonance Model Delta Wing

By

H. Hall

LONDON: HER MAJESTY'S STATIONERY OFFICE

1956

THREE SHILLINGS NET

U.D.C. No. 533.6.013.422:533.691.13

Technical Note No. Structures 149

January, 1955

ROYAL AIRCRAFT ESTABLISHMENT

Flutter calculations on a resonance model
delta wing

by

H. Hall

SUMMARY

Resonance tests on a dural model delta wing are used as a basis for flutter calculations to determine the effect on the flutter characteristics of changes in structural inertias and stiffnesses. Forward movement of the inertia axis and increased stiffness of the wing spars are shown to be separately beneficial.

The calculated flutter speeds are compared with flutter speeds given by formulae derived from earlier flutter tests on model delta wings in the wind tunnel and on ground launched rockets. There is qualitative agreement on the effects of the structural changes, but the absolute values of flutter speed differ appreciably. Possible explanations for the differences are discussed.

LIST OF CONTENTS

	<u>Page</u>
1 Introduction	3
2 Experimental data	3
2.1 Description of model	3
2.2 Method of variation of structural parameters	4
2.3 Calculation of structural inertia coefficients	4
3 Theoretical aerodynamic data	4
3.1 Determination of aerodynamic coefficients	4
3.2 Application of derivatives	5
4 Calculations and results	5
4.1 Details of calculation	5
4.2 Orthogonality of the modes	6
4.3 Results	7
4.4 Comparison with wind tunnel results	7
4.5 Comparison with rocket results	8
5 Conclusions	9
Acknowledgment	
References	

LIST OF ILLUSTRATIONS

	<u>Figure</u>
Outline of resonance model delta showing rib positions and mass distribution for standard inertia condition (inertia axis at 50% chord)	1
Wing fundamental and torsion modes for standard inertia, original spars case. Nodal lines and modal shapes.	2 2(a)
Wing fundamental and torsion modes for 40% inertia axis, original spars case. Nodal lines and modal shapes.	3 3(a)
Wing fundamental and torsion modes for standard inertia, stiffer spars case. Nodal lines and modal shapes.	4 4(a)
Chordwise distortion associated with the mode at 65 c.p.s., standard inertia and stiffer spars case.	5

1 Introduction

The effects of variation of inertias and stiffnesses on the normal modes of a delta wing have been investigated by resonance testing a dural model wing¹. The model, which represented only the structural properties of a typical delta aircraft, could not be flutter tested, but calculations have been made, based on the measured modes, to investigate the effects of changes in inertia and stiffness on the flutter characteristics.

This note gives the results of the flutter calculations. The effect of inertia variations on the resonance modes was originally investigated by Gaukroger². Some of Gaukroger's measurements were later repeated by Webb¹, who also extended the measurements to cover the effect of replacing the original spars by two alternative sets of stiffer spars. The results for the stiffest set of spars have not been used as they were not considered to be sufficiently accurate; it was thought that, for frequencies above 60 c.p.s., a true mode was not being obtained because of undue flexibility at the fuselage rib.

In the calculations use has been made of the aerodynamic derivatives calculated by Woodcock for a delta wing³, and their application to the various modes is shown.

This investigation is compared with two earlier investigations which had the same object but employed different means, namely, the direct determination of the effects of structural changes on the flutter of model delta wings in the wind tunnel⁴ and on ground launched rockets⁶. The resonance model delta was larger and more representative of a full scale structure, but on the other hand calculation of the flutter characteristics is of course less reliable than actual flutter tests.

The general conclusion which can be drawn from this comparison is that there is satisfactory qualitative agreement between flutter test and calculation results. An unusual feature is however, that the flutter test results give lower critical flutter speeds than the calculated; some possible reasons for this are discussed later in the note.

2 Experimental data

2.1 Description of model

The model was made of dural and represented a tailless cropped delta of approximately 11 ft span and 5 ft root chord. Fig. 1 shows the model and its relevant dimensions. The structure was supported internally by five ribs on each side running in a chordwise direction. The fuselage was represented by the hollow centre piece of constant cross-section, between the two inner ribs of each wing.

In the design of the model, the aim was to achieve flexural and torsional wing stiffness distributions that were representative of full scale. The overall value of the stiffness ratio finally used was, with the original set of spars fitted.

$$\frac{\text{Flexural stiffness } I_{\phi}}{\text{Torsional stiffness } m_{\theta}} = 2.5 \text{ measured at } 0.7 \text{ span.}$$

Considerable flexural stiffness was provided by the skin itself, which included that provided by the stringers in full scale design. The leading and trailing edges of the wing may be considered as spars, so that the construction was normal except that the two spars were further apart than they would be in practice.

The model was supported at points at the nose and tail of the fuselage. Excitation was by means of an inertia exciter which could be attached at various points on the fuselage.

2.2 Method of variation of structural parameters

Wooden blocks were fitted internally in the fuselage and their positions could be adjusted to give any desired overall c.g. position without affecting the total mass; these blocks also formed convenient attachment points for the exciter. Wing masses were represented by lead strips fitted along the four outboard ribs of each wing to the top and bottom surfaces, and inertia axis position was varied by changing the positions of these strips. Stiffness variations were effected by changing the spars.

2.3 Calculation of structural inertia coefficients

The inertia of the model was represented by a system of masses placed at various points on the wing and fuselage (Fig. 1). These point mass positions had previously been calculated to give the correct overall c.g. position and inertia axis.

Nodal lines for the particular modes obtained for three inertia and stiffness configurations are shown in Figs. 2, 3 and 4. Their application to the determination of the inertia coefficients was as follows. The reference axis was taken at the mid chord and the reference section that of the 5th rib which is distant l , say, from the centre line. This choice of reference axis was convenient when determining the aerodynamic coefficients, because Woodcock's derivatives were referred to this axis.

Then if $f_1(\eta)$ represents the downward displacement of the reference axis in the i th mode and $F_1(\eta)$ the nose up twist about this axis in the same mode, the structural inertia coefficients are given in the usual manner by

$$A_{rr} = \sum \{ m l^2 f_r^2 + 2 m x l f_r F_r + m x^2 F_r^2 \}$$

and

$$A_{rs} = \sum \{ m l^2 f_r f_s + m x l (f_r F_s + f_s F_r) + m x^2 F_r F_s \}$$

where m is any point mass.

x is its distance aft of the mid-chord axis

$m x$ is its mass moment about the reference axis

$m x^2$ is its moment of inertia about the reference axis

3 Theoretical Aerodynamic Data

3.1 Determination of Aerodynamic coefficients

In Woodcock's notation³ the aerodynamic coefficients in the equations of motion are defined to be

$$c_{rs} = (Z_z)_{rs} + (Z_\alpha)_{rs} + (A_z)_{rs} + (A_\alpha)_{rs}$$

$$b_{rs} = (Z_{\dot{z}})_{rs} + (Z_{\dot{\alpha}})_{rs} + (A_{\dot{z}})_{rs} + (A_{\dot{\alpha}})_{rs}$$

where the aerodynamic inertias are included in the stiffness terms. The functions Z and A are defined as

$$(Z_z)_{ij} = (l_z)_{ij} \int_0^1 f_i(\eta) \cdot f_j(\eta) d\eta; (A_z)_{ij} = (-m_z)_{ij} \int_0^1 \left(\frac{c}{s}\right) F_i(\eta) \cdot f_j(\eta) d\eta$$

$$(Z_\alpha)_{ij} = (l_\alpha)_{ij} \int_0^1 \left(\frac{c}{s}\right) f_i(\eta) F_j(\eta) d\eta; (A_\alpha)_{ij} = (-m_\alpha)_{ij} \int_0^1 \left(\frac{c}{s}\right)^2 F_i(\eta) F_j(\eta) d\eta$$

the Z_z , A_z etc are of the same form but depend on the dotted derivative and are multiplied inside the integral by the factor $\left(\frac{c}{c_{in}}\right)$. In the present case

the reference section is taken at the fifth rib and the limits of integration are correspondingly modified. The equivalent constant derivatives, which are constant over the span, for use in these functions depend on a set of known equivalent constant derivatives associated with a set of arbitrary modes of the type $\hat{F}_1(\eta) = |\eta|^1$, $\hat{F}_i(\eta) = |\eta|^1$ where i has integral values from 0 to 4. The mid chord flexure and torsion modes are represented as linear functions of these arbitrary modes and are used in this form to determine the aerodynamic derivatives. In the present work a frequency parameter, based on the mean chord, of 0.26 was assumed when evaluating the derivatives. This was in fairly good agreement with the value of 0.11 and 0.15 obtained on solution of the flutter equations.

3.2 Application of Derivatives

Woodcock's derivatives³ were calculated for a cropped delta of aspect ratio 3 with leading edge sweepback of 45° whereas in the particular model delta under consideration the aspect ratio is 3.5 and the sweepback also 45°. Despite the somewhat higher aspect ratio, it is unlikely that the results will be seriously affected since the aerodynamic coefficients have been determined by using the equivalent constant derivatives as suggested by Woodcock. A further point of difference between theory and practice is that the resonance model delta is cropped at the apex of the delta. This is not likely to affect the lift distribution or the centre of pressure position markedly, and the effect on the aerodynamic coefficients has been ignored.

In calculating the derivatives Woodcock considered only two chordwise collocation points so that the effect of chordwise distortion was not allowed for. In the practical modes obtained however, appreciable chordwise distortion is associated with all the torsion modes, mostly over the inboard portions of the wing (Fig. 5). This distortion has been ignored by taking the chordwise strips to be rigid; thus the vertical displacements of points on such a strip have been represented by joining the leading and trailing edge displacements by a straight line. In fact it seems likely that such distortion might affect the aerodynamic characteristics appreciably and if it were taken into account by applying W.P. Jones's method⁵ with three or more collocation points, might have a considerable effect on the critical speeds.

- Case 1 Original spars and standard inertia condition i.e. overall c.g. at 50% root chord, inertia axis at 50% chord.
- Case 2 Original spars, inertia axis at 40% chord.
- Case 3 Stiffer spars, standard inertia condition.

The analysis for a typical case (Case 2) is as follows. The normal translation along the mid chord axis and incidence of fore and aft sections of the fundamental mode at 14.8 c.p.s. can be represented by the displacement functions

$$f_1 = -0.6155 + 2.9429\eta - 15.1128\eta^2 + 30.0724\eta^3 - 16.2871\eta^4$$

$$F_1 = 1.2931 - 7.3908\eta + 37.7078\eta^2 - 73.8865\eta^3 + 47.2374\eta^4$$

and similarly for the torsion mode at 63.2 c.p.s.

$$f_2 = 1.5871 + 20.3591\eta - 133.8368\eta^2 + 219.3898\eta^3 - 106.4989\eta^4$$

$$F_2 = 6.4871 - 71.9149\eta + 283.0323\eta^2 - 514.8042\eta^3 + 261.5562\eta^4$$

The coefficients in these equations are then used in conjunction with the equivalent constant derivatives for the known set of modes of type $|\eta|^n$ to determine a set of derivatives. This leads to the following set of aerodynamic coefficients.

$$c = \begin{bmatrix} 0.05694 & -2.1626 \\ 1.3916 & -20.3369 \end{bmatrix} \quad b = \begin{bmatrix} 0.4425 & -0.4875 \\ 1.6956 & 15.9432 \end{bmatrix}$$

The structural inertias are worked out as described in section 2.3 and in the non-dimensional form are given by

$$a = \begin{bmatrix} 22.5369 & -1.8581 \\ -1.8581 & 470.3878 \end{bmatrix}$$

The elastic matrix is derived from the inertias and frequencies as

$$e = e_{11} \begin{bmatrix} 1 & 0 \\ 0 & r \end{bmatrix} \quad \text{where } e_{11} = \frac{a_{11} \omega_1^2 C^2}{V^2} \text{ and } r = \frac{a_{22}}{a_{11}} \left(\frac{\omega_2}{\omega_1} \right)^2$$

No variable was taken in the calculations and the solution was obtained directly for speed and frequency parameter. Anything corresponding to a physical change, such as masses placed on the wing to represent various fuel tank conditions, would be expected to affect the modes obtained and the corresponding flutter speeds accordingly.

4.2 Orthogonality of the Modes

The reference axis for defining the position of the point masses on the wing was chosen as the line passing through the overall c.g. position. The products of inertia of the modes with pitch about the c.g. are reasonably small in most cases. As examples, two of the cases considered are quoted.

Case 2. The products of inertia between pitch and each of the fundamental and torsion modes are small and the cross inertia between these two modes is also small.

Case 3. The product of inertia between pitch and the fundamental mode is of the order of 22%. This would seem to indicate that a true normal mode had not been measured. The cross inertia between fundamental and torsion modes here is large and of the order of 70%.

4.3 Results

The critical speeds obtained relate directly to a model of the dimensions given, but some comparison with other results can be obtained from the formulae mentioned later. The following are the results obtained.

Case 1. $V_c = 4,106$ ft/sec, $\nu = 0.11$; if the cross inertia, which should ideally be zero, is neglected then $V_c = 4,284$ ft/sec, $\nu = 0.10$.

Case 2. $V_c = 4,547$ ft/sec, $\nu = 0.15$.

Case 3. No solution for V_c i.e. no flutter is obtained in this case.

In Cases 1 and 3 there are large cross inertias present, and the flutter speed might be expected to be sensitive to this factor. In fact however, when the cross-inertia was put equal to zero in Case 1, a relatively small increase in V_c was obtained. The cross inertia in Case 2 is however, already small.

There is an element of uncertainty about the aerodynamic coefficients used in the calculations. The representation of the actual set of mid chord modes obtained in terms of the arbitrary set of modes $f_i(\eta)$ and $F_i(\eta)$ for integral values of i is not accurate in all cases. A better set of results might be obtained if the method were extended for larger values of i . It is difficult to assess the change which any such modification might bring about in the final results.

4.4 Comparison with Wind Tunnel Results

In his report on the wind tunnel tests of a delta wing⁴, Gaukroger correlates his results with the torsional stiffness requirements of A.P.970 by plotting values of the stiffness parameter involved against various ratios of fuselage to wing moment of inertia for several inertia axis positions. An estimate of flutter speed can be obtained for any delta of approximately the same planform using known values of torsional stiffness and wing dimensions. This method has been applied to the resonance model delta.

$$\text{The formula for flutter speed is } \frac{1}{V_c} \left(\frac{m_\theta}{d c_m^2} \right)^{\frac{1}{2}} = k \quad (1)$$

where V_c is the critical flutter speed

m_θ is the wing torsional stiffness measured at 0.7s

$d = 0.9s$

$c_m =$ wing mean chord

k is the parameter for which Gaukroger quotes experimental results, its value depending on the ratio of pitching moments of inertia of fuselage and wing (See Fig. 7, Ref. 4).

Application of the formula to the resonance model delta gives the following results

Case 1. $k = 0.0148$, $V_c = 3,296$ ft/sec ($m_\theta = 1,476, 800$ lb in./rad)

Case 2. $k = 0.0140$, $V_c = 3,484$ ft/sec ($m_\theta = 1,476$, 800 lb in/rad)

Case 3. $k = 0.0148$, $V_c = 3,603$ ft/sec ($m_\theta = 1,765$, 200 lb in/rad)

The calculated results appear to be optimistic when compared with those obtained from the wind tunnel tests e.g. the calculated results show that the critical speed for the 40% inertia axis case is 10.7% above that for the standard inertia case (Cases 2 and 1) whereas the wind tunnel test formula (1) gives a corresponding increase of only 5.7%; the overall values of the calculated results are also higher than those from the wind tunnel tests. The following points may be considered in assessing the relative values of the two sets of results.

(1) As stated before, the resonance model delta was considered to be more representative of a full scale structure than the single spar model used to investigate similar inertia variations in the wind tunnel. Some difference in the results may therefore be due to the differences in structure.

(2) A further difference in the two models is that the ratio of flexural to torsional stiffness of the wind tunnel delta was 6:1 whereas that of the resonance model was 2.5:1. This may account for the lower speeds given by the wind tunnel results.

(3) In the flutter calculations no account has been taken of any body freedoms which the model might have in flight except those which are implicit in the fundamental and torsion modes considered. The wind tunnel test model was allowed body freedoms in pitch and vertical translation so that strictly the results for the resonance delta obtained from the wind tunnel formula (1) are not comparable with the calculated values. The values of the parameter k for the three resonance model cases, however, do not vary much (between -0.5% and -3%) from those obtained by Gaukroger⁴ for the corresponding fixed root conditions; hence, it is unlikely that any major part of the discrepancy in the results can be accounted for by the neglect of the body freedoms in the calculations.

(4) No reliable information about the higher frequency modes of the resonance model, particularly the first overtone torsion mode, was available, and as has been noted in section 4.1, it was hoped that the binary flutter calculations would give the relative critical speeds sufficiently accurately. It is possible, however, that the inclusion of this mode in the calculations could reduce the critical speeds, which would then be in closer agreement with those predicted from formula (1).

The fact that no solution was obtained for critical speed in the case of the stiffer spars and standard inertia condition (Case 3) could be due to the fact that the nodal line in the fundamental mode is further outboard than in the other cases (see Fig. 4) and the coupling between the modes is consequently reduced. This particular result might be altered by the introduction of further modes and body freedoms.

4.5 Comparison with rocket results

From flutter texts on delta wings using ground launched rockets, Molyneux and Ruddlesden⁶ suggest the following formula for determining the flutter speed of a delta wing

$$V_1 = \left(\frac{m_\theta}{\rho_0 s c_m^2} \right)^{\frac{1}{2}} \frac{(0.9 - 0.33k) (0.77 + \frac{0.1}{r}) (0.95 + \frac{0.1}{\sigma w})}{0.78 (g - 0.1)} \text{Sec}^{\frac{3}{2}} \left(\Lambda - \frac{\pi}{16} \right) \quad (2)$$

where the symbols are defined in Ref. 6.

The value of V_1 is then modified by a Mach number correction factor $(1 - 0.166 M_1 \text{ Cos}\Delta)$ to give the required flutter speed.

Since the calculations on the resonance model delta used derivatives for incompressible flow, the only valid comparison to be made between the rocket test and calculated values is that between V_1 and the calculated speeds. The values of V_1 from the formula (2) for the three resonance model cases are as follows

	<u>Rocket tests</u> Formula (2)	<u>Wind Tunnel Tests</u> Formula (1)	<u>Calculation</u>
Case 1	$V_1 = 3000 \text{ ft/sec}$	$= 3296 \text{ ft/sec}$	$= 4,106 \text{ ft/sec}$
Case 2	$V_1 = 4000 \text{ ft/sec}$	$= 3484 \text{ ft/sec}$	$= 4,547 \text{ ft/sec}$
Case 3	$V_1 = 3352 \text{ ft/sec}$	$= 3603 \text{ ft/sec}$	$= \infty$

The 40% inertia axis case (Case 2) shows an increase of $33^{1/3}\%$ in flutter speed over the standard inertia case (Case 1) as compared with 10.7% from the calculated values. The case 1 value compares favourably with the wind tunnel test value but not with calculation, whilst the case 2 value is mid-way between the values predicted from the wind tunnel tests and calculation. The increase in the flutter speed due to the stiffer spars (Cases 1 and 3) is less than that due to forward movement of the inertia axis (Cases 1 and 2), a reversal of the corresponding effects shown by the other two sets of values.

The reasons for these differences are not precisely known. The rocket test results covered a wide variation in stiffness ratio so that this factor has been allowed for in the formula (2). Some difference may result from the fact that the rocket wings are of different construction from the wind tunnel and resonance models.

A better comparison can be obtained if the inertia axis term $1/(g - 0.1)$ in formula (2) is replaced by 3.19 (1.4-g). This gives the same value for V_1 at $g = 0.42$ but lower values of $g < 0.42$ and higher values for $g > 0.42$. With this modification the flutter speeds for the resonance model by formula (2) would be

Case 1.	$V = 3445 \text{ ft/sec.}$
Case 2.	$V = 3828 \text{ ft/sec.}$
Case 3.	$V = 3849 \text{ ft/sec.}$

The 40% inertia axis case then gives a flutter speed 11.1% over the basic case, similar to the calculated results, although here again the absolute calculated values are still higher. The general agreement with the calculated and wind tunnel test values is much better, however, and from this particular investigation the suggested modification to formula (2) would be desirable.

5 Conclusions

The design implications of the investigation are that the flutter speed of a delta wing will be increased by moving the inertia axis forward or by increasing the stiffness of the spars. These general conclusions

used for the wind tunnel investigation had a much higher stiffness ratio (flexure to torsion) than the resonance model, and secondly that the models used in both the wind tunnel and the rocket investigations were of much simpler construction than the resonance model. The effect of higher frequency modes has been neglected in the calculations and it is possible that, if these were accurately known and could consequently be taken into account in the calculations, the flutter speeds would compare much more favourably in absolute value with those predicted using the formulae (1) and (2). It is unlikely that any major part of the discrepancy in the results can be accounted for by the neglect of the body freedoms in the calculations.

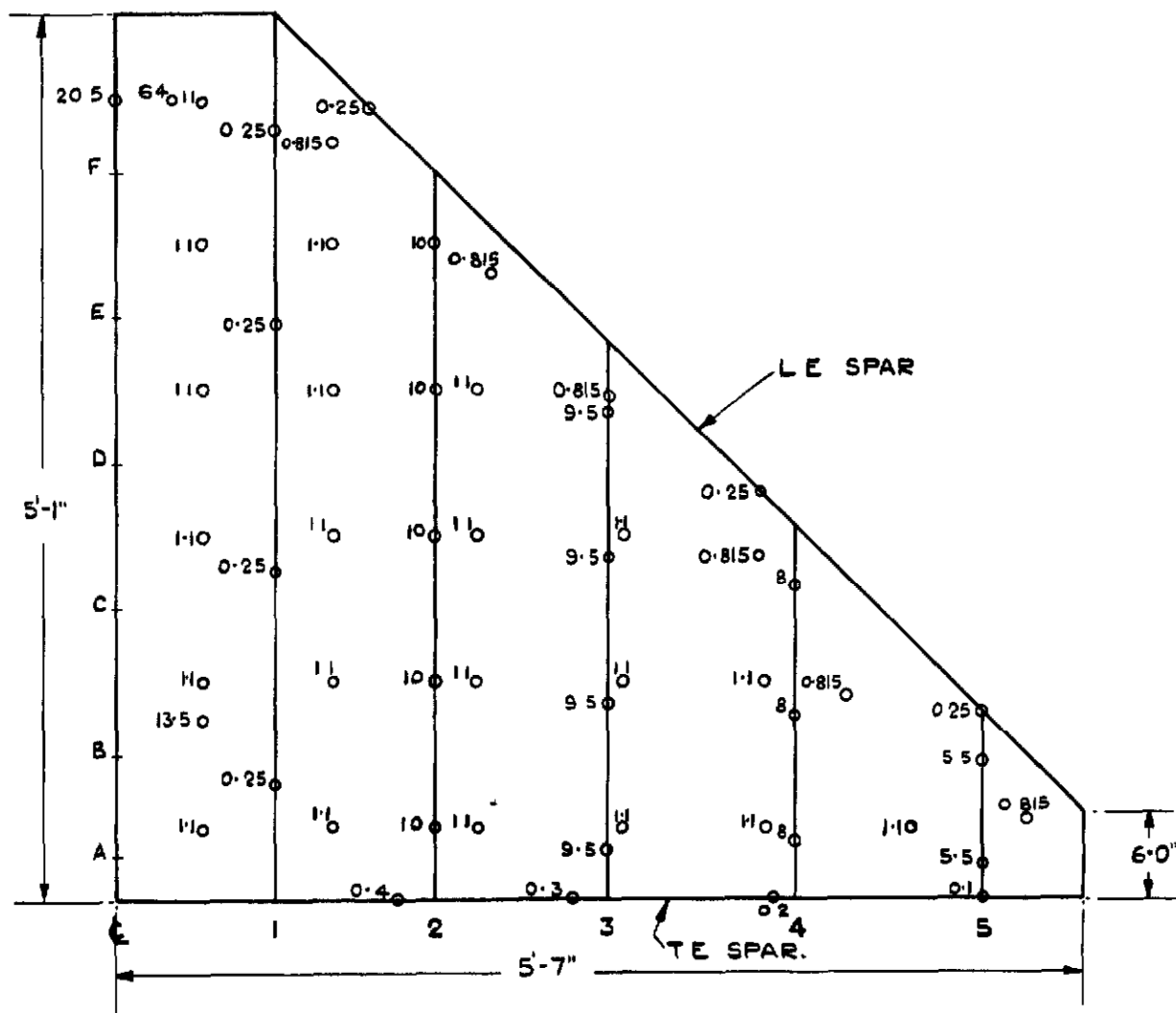
It is considered also that the discrepancies are probably partly due to the neglect, in the calculation of the aerodynamic coefficients in the present investigation, of the chordwise distortion in the measured modes of the resonance model. The assumption of a linear displacement mode between leading and trailing edges is questionable, and a possibly better approximation would be to take the tangent line at the three-quarter chord position.

Acknowledgment

The author wishes to acknowledge the assistance of Mrs. V.M. Longden who performed much of the computational work involved in this note.

REFERENCES

<u>No.</u>	<u>Author</u>	<u>Title, etc.</u>
1	D.R.B. Webb	R.A.E. Report to be issued
2	D.R. Gaukroger	Natural frequencies and modes of a model delta aircraft. R & M. 2762 January, 1950
3	D.L. Woodcock	Aerodynamic derivatives for a delta wing Oscillating in Elastic Modes C.P.170 July, 1952
4	D.R. Gaukroger, E.W. Chapple, A. Milln.	Wind Tunnel Flutter Tests on a Model Delta Wing under Fixed and Free Root Conditions R & M 2826 September, 1950
5	W.P. Jones	The calculation of aerodynamic derivative coefficients for wing of any planform in non-uniform motion. R & M 2470 December, 1946
6	W.G. Molyneux, F. Ruddlesden	Flutter tests on some delta wings using ground launched rockets. R.A.E. Report Structures 173 January, 1955 A.R.C. 17,752.



A, B, C, --- F ARE CHORDWISE STATIONS AT WHICH PICK-UPS ARE LOCATED.

**FIG. I. OUTLINE OF RESONANCE MODEL DELTA
SHOWING RIB POSITIONS AND MASS
DISTRIBUTION FOR STANDARD
INERTIA CONDITION.
(INERTIA AXIS AT 50% CHORD.)**

NODAL LINES.

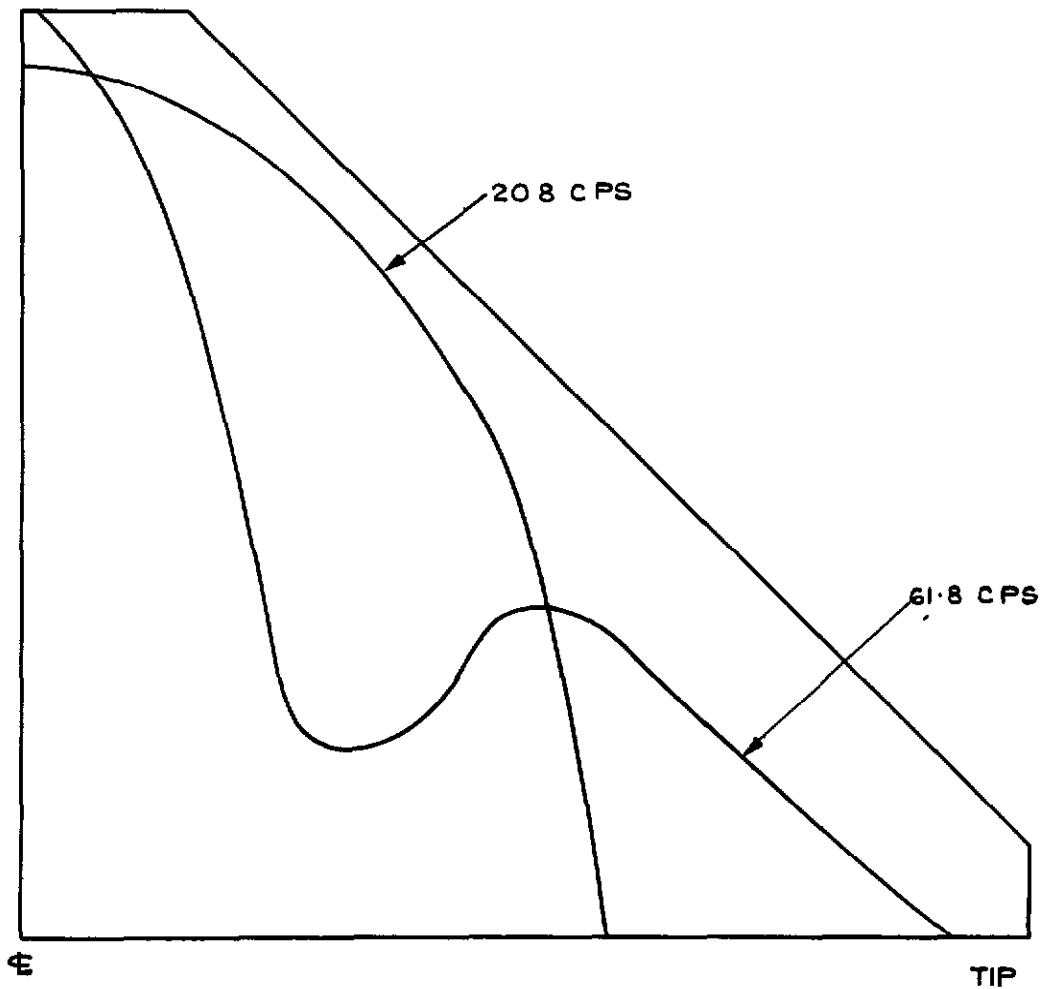
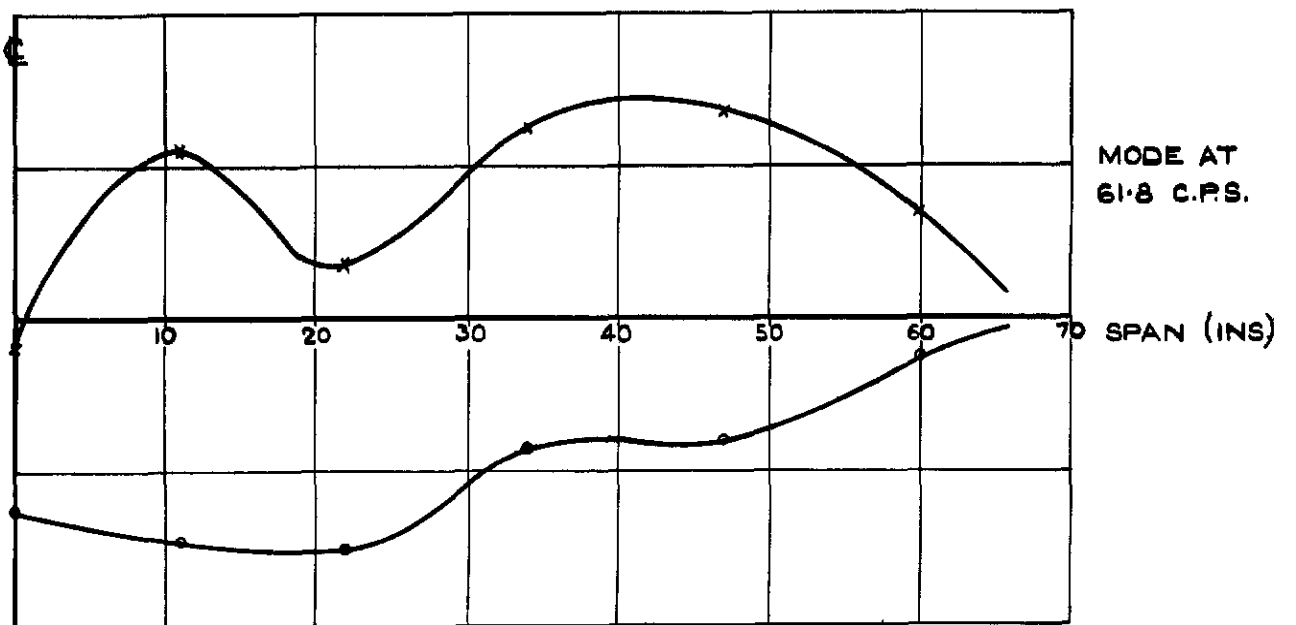
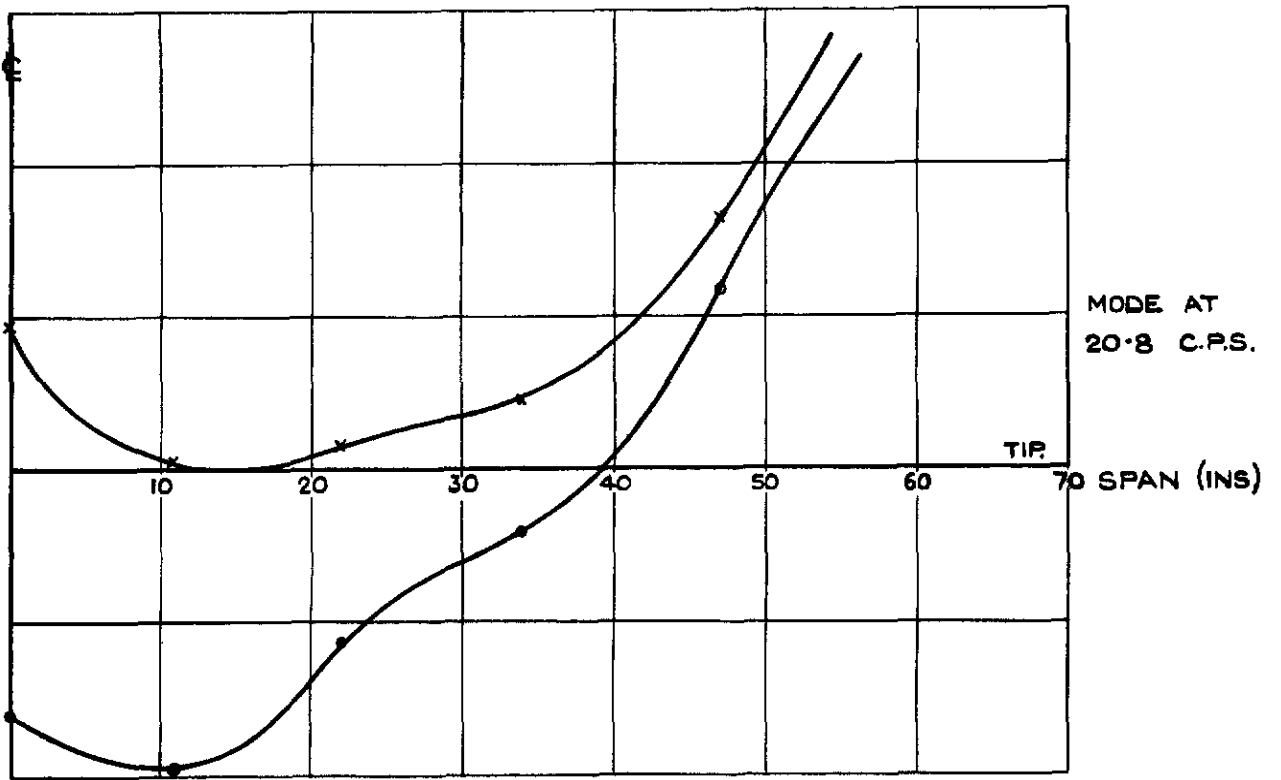
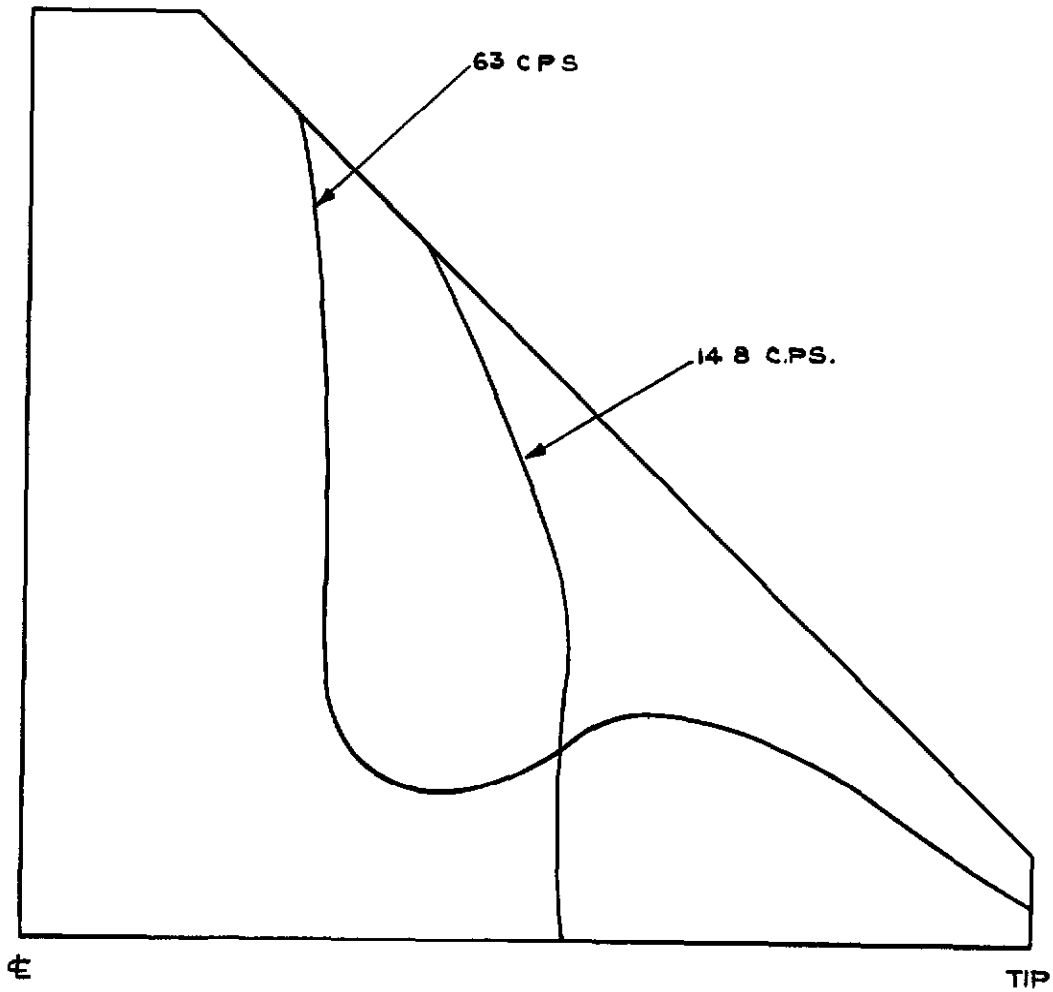


**FIG. 2. WING FUNDAMENTAL AND TORSION
MODES FOR THE STANDARD INERTIA,
ORIGINAL SPARS CASE**

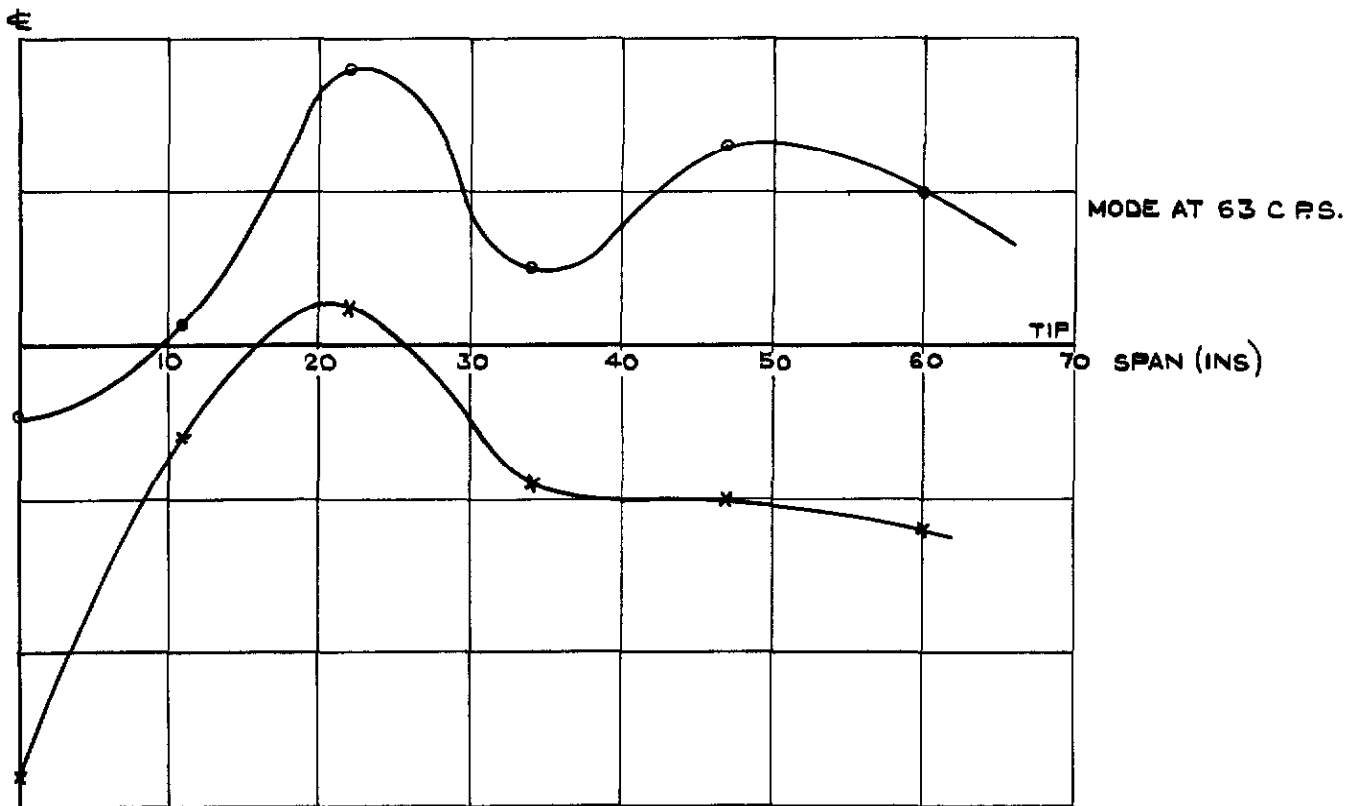
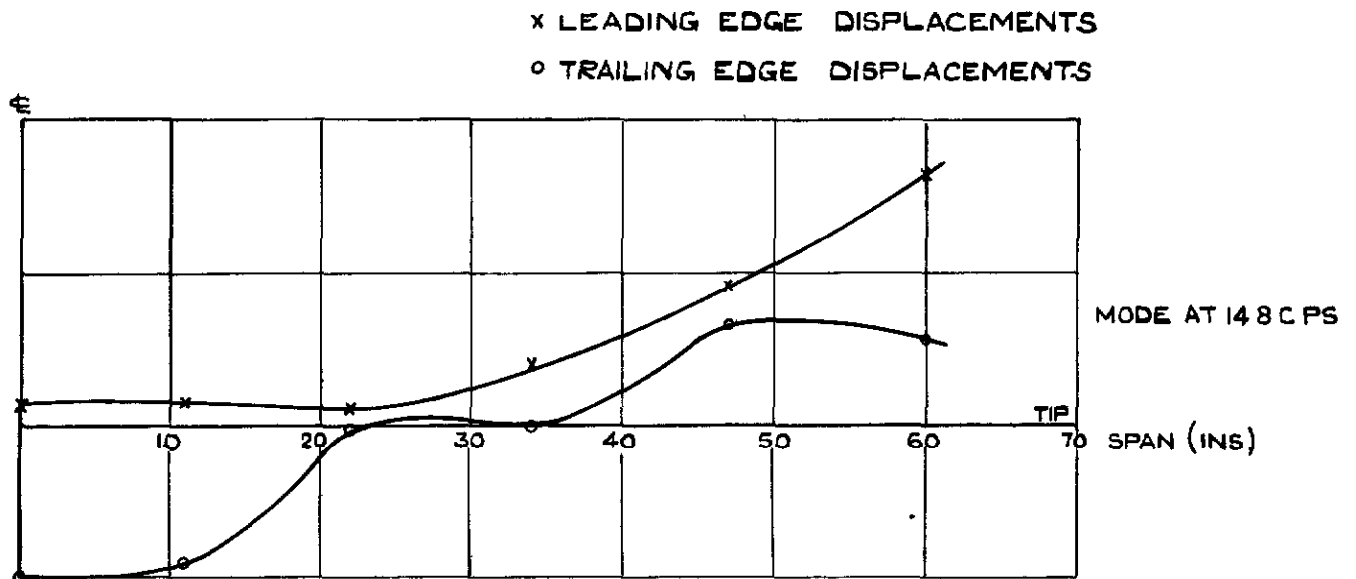
x LEADING EDGE DISPLACEMENTS
o TRAILING EDGE DISPLACEMENTS



NODAL LINES

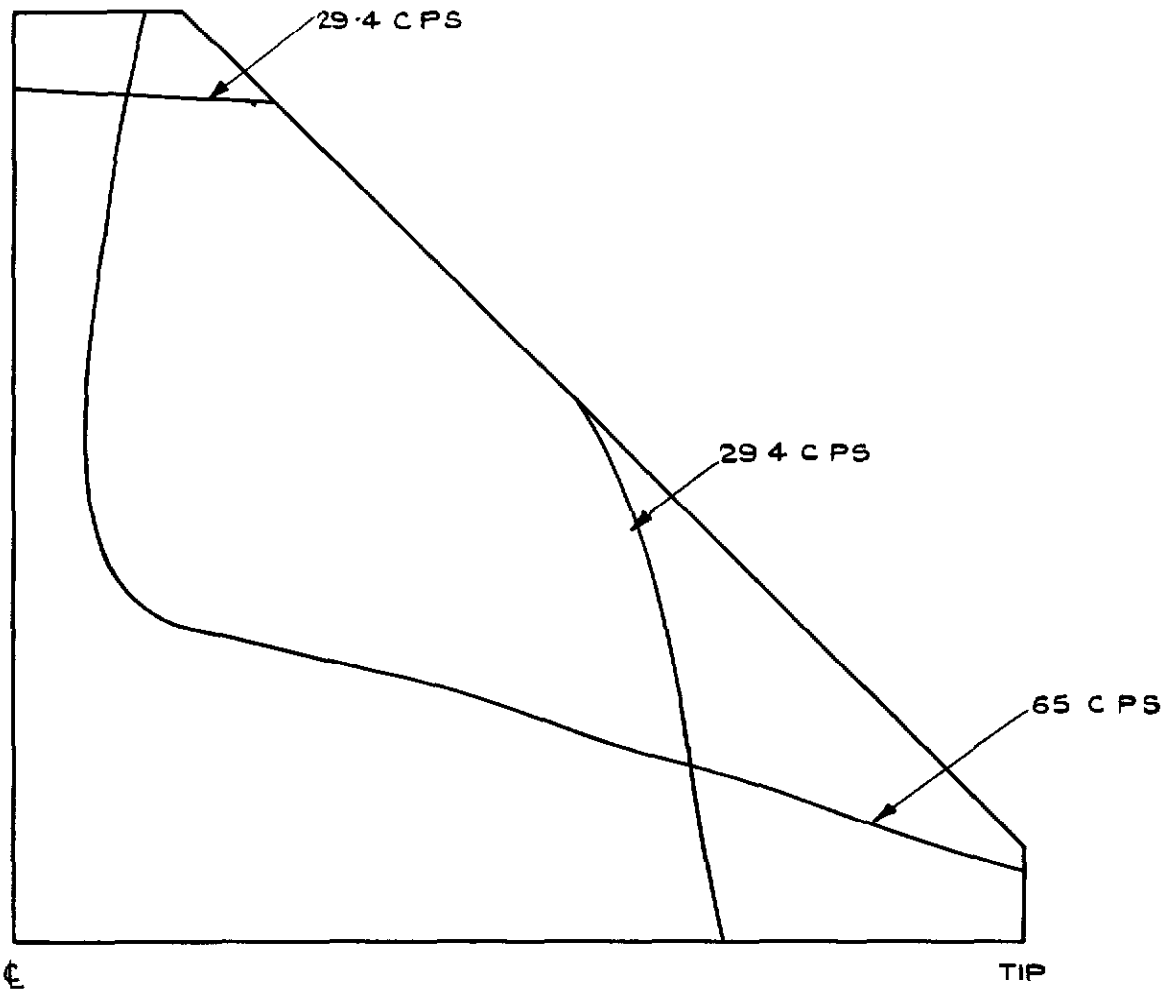


**FIG. 3. WING FUNDAMENTAL AND TORSION
MODES FOR 40% INERTIA AXIS,
ORIGINAL SPARS CASE.**



**FIG. 3 (a) WING FUNDAMENTAL & TORSION
 MODES FOR 40% INERTIA AXIS,
 ORIGINAL SPARS CASE.
 MODAL SHAPES.**

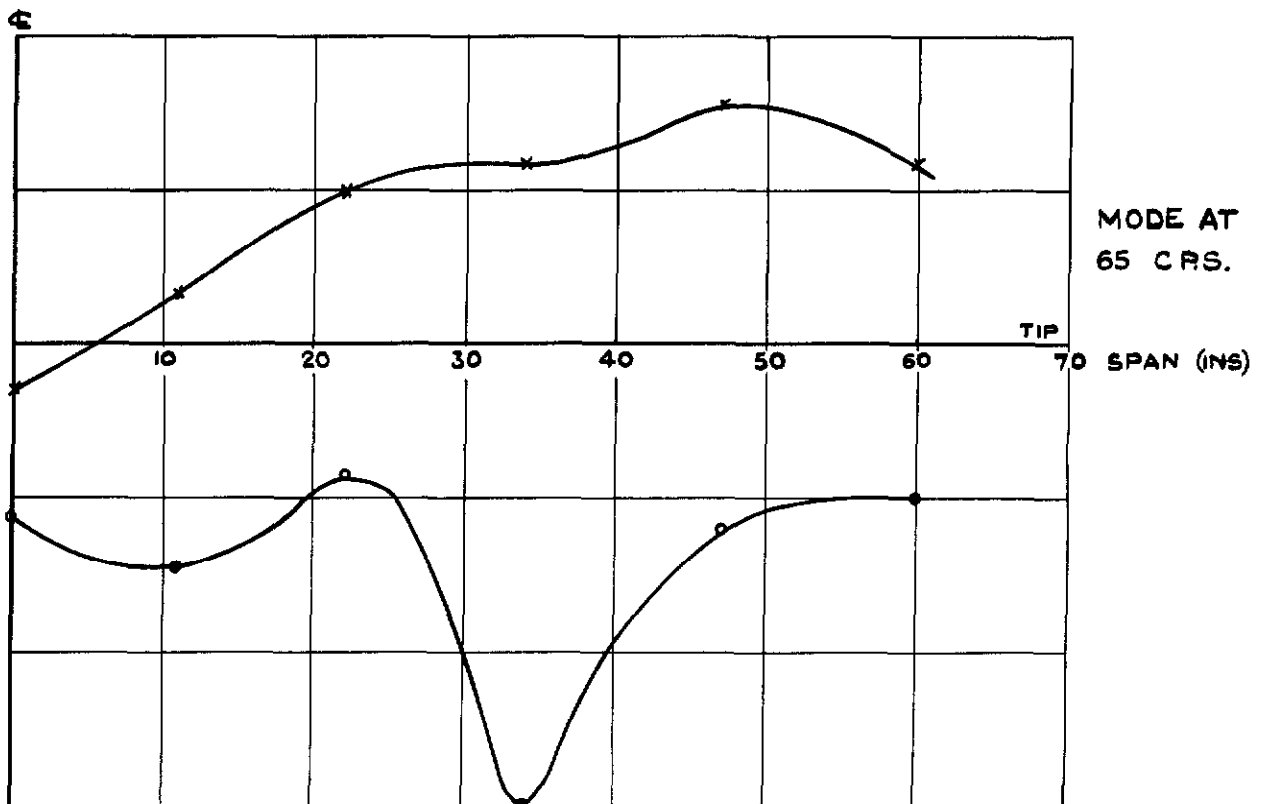
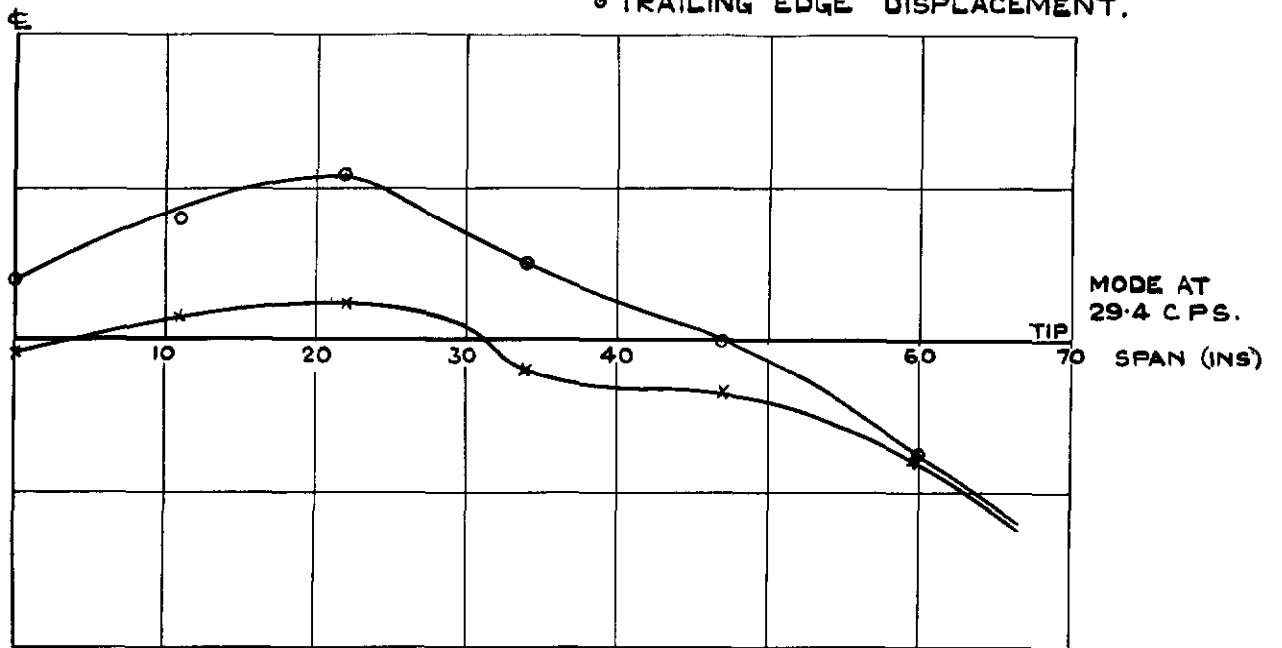
NODAL LINES.



**FIG. 4. WING FUNDAMENTAL AND TORSION
MODES FOR STANDARD INERTIA,
STIFFER SPARS CASE.**

x LEADING EDGE DISPLACEMENT

o TRAILING EDGE DISPLACEMENT.



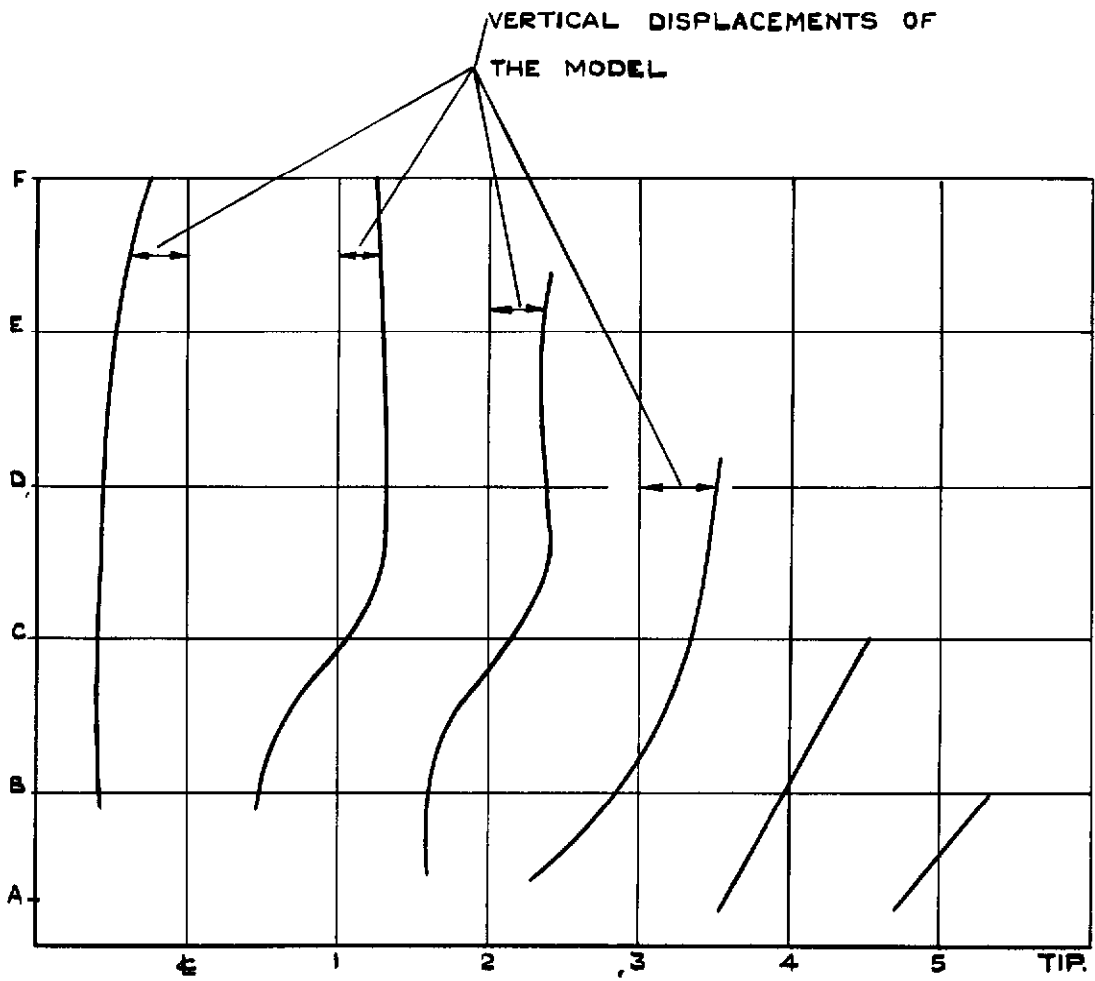


FIG. 5. CHORDWISE DISTORTION ASSOCIATED WITH MODE AT 65 C.P.S. STANDARD INERTIA & STIFFER SPARS CASE.

Crown copyright reserved

Published by

HER MAJESTY'S STATIONERY OFFICE

To be purchased from

York House, Kingsway, London W C 2

423 Oxford Street, London W. 1

P O Box 569, London S E 1

13A Castle Street, Edinburgh 2

109 St Mary Street, Cardiff

39 King Street, Manchester 2

Tower Lane, Bristol 1

2 Edmund Street, Birmingham 3

80 Chichester Street, Belfast

or through any bookseller

PRINTED IN GREAT BRITAIN